Environmental Science & Technology

pubs.acs.org/est

Article

High Gaseous Nitrous Acid (HONO) Emissions from Light-Duty Diesel Vehicles

Songdi Liao, Jiachen Zhang, Fei Yu, Manni Zhu, Junwen Liu, Jiamin Ou, Huabin Dong, Qinge Sha, Zhuangmin Zhong, Yan Xie, Haoming Luo, Lihang Zhang, and Junyu Zheng*

Cite This: *Environ. Sci. Technol.* 2021, 55, 200−208

Read Online

ACCESS | Metrics & More | Article Recommendations | Supporting Information

ABSTRACT: Nitrous acid (HONO) plays an important role in the budget of hydroxyl radical (•OH) in the atmosphere. Vehicular emissions are a crucial primary source of atmospheric HONO, yet remain poorly investigated, especially for diesel trucks. In this study, we developed a novel portable online vehicular HONO exhaust measurement system featuring an innovative dilution technique. Using this system coupled with a chassis dynamometer, we for the first time investigated the HONO emission characteristics of 17 light-duty diesel trucks (LDDTs) and 16 light-duty gasoline vehicles in China. Emissions of HONO from LDDTs were found to be significantly higher than previous studies and gasoline vehicles tested in this study. The HONO emission factors of LDDTs decrease significantly with stringent control standards: 1.85 ± 1.17, 0.59 ± 0.25, and 0.15 ± 0.14 g/kg for China III, China IV, and China V, respectively. In addition, we found poor correlations between HONO and NOx emissions, which indicate that using the ratio of HONO to NOx emissions to infer HONO emissions might lead to high uncertainty of HONO source budget in previous studies. Lastly, the HONO emissions are found to be influenced by driving conditions, highlighting the importance of conducting on-road measurements of HONO emissions under real-world driving conditions. More direct measurements of the HONO emissions are needed to improve the understanding of the HONO emissions from mobile and other primary sources.

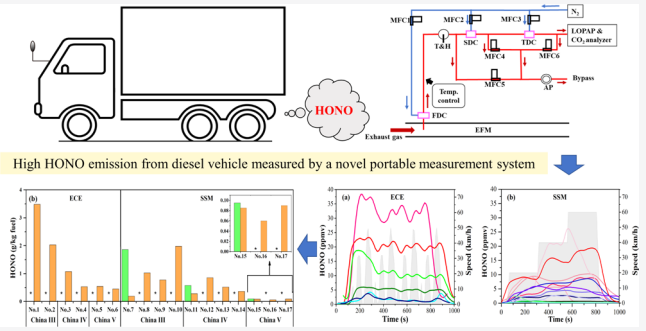

INTRODUCTION

Gaseous nitrous acid (HONO) is an important precursor of hydroxyl radical (•OH),[1−3] an important oxidant that acts as a detergent for most pollutants and influences ozone formation in the troposphere.[4−6] Although the roles of HONO in the tropospheric photochemistry have been widely investigated, the sources of HONO remain not fully understood.[7−9] Previous studies suggested that HONO may arise from homogeneous reactions in the atmosphere,[10] heterogeneous reactions of nitrogen dioxide (NO_2) on surfaces,[11] soil emissions by microbial activities,[12] and direct vehicular emissions.[13] However, air quality models accounting for all these sources cannot reproduce the full scale of HONO concentrations.[14] The observed HONO concentrations were about 2 times higher than model estimates,[15] suggesting that some sources of HONO were either missing or greatly underestimated. Recent efforts have been made to improve the understanding of the HONO emissions from soil;[16,17] however, there continues to be a scarcity of HONO emission measurements from mobile sources.

Several studies have identified vehicle exhaust as the most important source for direct HONO emissions in urban areas, which contributes to 12−49% of the atmospheric HONO burden during nighttime and early morning.[18−21] Due to the lack of measurement data on emission factors (EFs) of HONO from mobile sources, the ratio of HONO emissions to NOx emissions ($ER_{HONO/NOx}$) is often used as a proxy to calculate primary HONO emissions from vehicles. $ER_{HONO/NOx}$ of 0.8%, which was established by Kurtenbach et al. (2001),[13] has been widely applied in vehicle emission estimation and modeling studies for HONO. The underlying assumption of using this ratio to infer HONO emissions is that HONO and NOx are well correlated, as observed in tunnel studies.[13,22] Nevertheless, a recent chassis dynamometer testing on gasoline vehicles found low correlation between HONO and NOx.[23] In fact, studies on vehicle emissions showed significant discrepancies in $ER_{HONO/NOx}$, a large range was found from 0.03 to 2.1%.[19,22−29] The large discrepancies of $ER_{HONO/NOx}$ between previous studies can be partially attributed to individual differences of the measured vehicles especially their fuels (gasoline and diesel). However, most previous studies focused

Received: August 19, 2020
Revised: November 20, 2020
Accepted: November 23, 2020
Published: December 8, 2020

https://dx.doi.org/10.1021/acs.est.0c05599
Environ. Sci. Technol. 2021, 55, 200−208

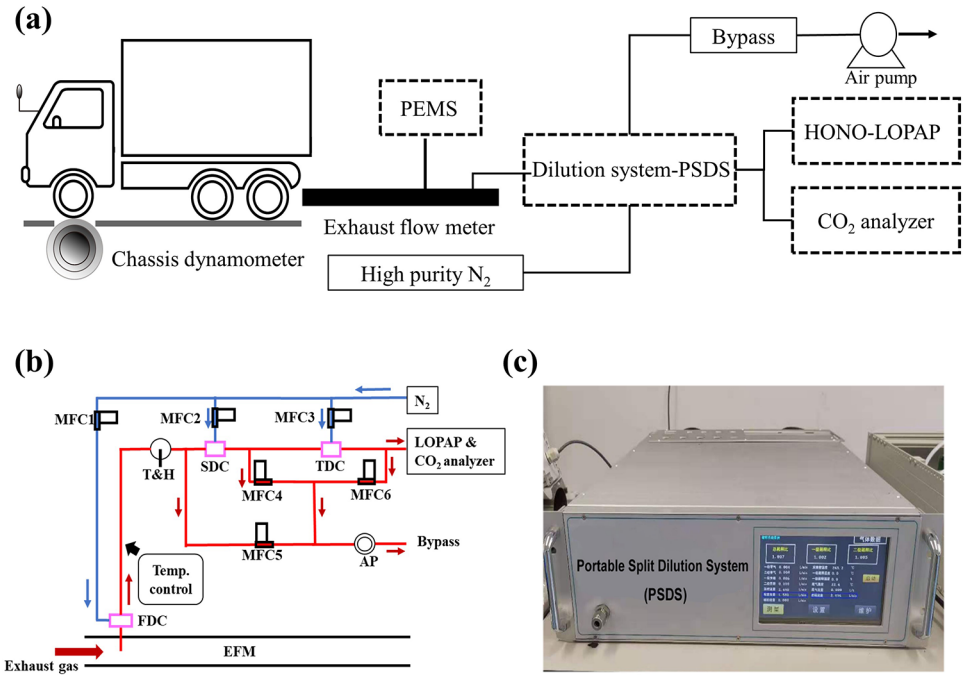

Figure 1. Schematic diagram of the vehicle chassis dynamometer (a). The tested vehicle is set on the chassis and the exhaust gas is diluted in PSDS for diesel vehicles by high-purity nitrogen through gas mass flowmeters. PSDS is connected with the vehicle tailpipe via an exhaust flow meter (EFM). The length of the tube connecting the tailpipe with EFM is approximately 3 m. Schematic diagram (b) and picture (c) of PSDS, consisting of first dilution chamber (FDC), second dilution chamber (SDC), third dilution chamber (TDC), mass flow controller (MFC1 to MFC6), air pump (AP), temperature and humidity sensor (T&H), exhaust flow meter (EFM), LOPAP-JNU, and CO_2 analyzer. The size (L × W × H) of the PSDS is 440 mm × 440 mm × 130 mm.

on HONO emissions from gasoline vehicles. Recently, Trinh et al. (2017)[27] found that HONO concentrations from diesel vehicle exhaust (868.8 ppbv) were 700 times higher than that from gasoline vehicles (1.2 ppbv). Although Trinh et al. (2017)[27] highlighted the potential of diesel vehicles as one of the most important sources of HONO, their results were only based on a single vehicle, making the results difficult to apply to a fleet with any certainty. However, it does highlight the likely importance in conducting additional HONO emission measurements from diesel vehicles.

Currently, many of the HONO emission measurements are fleet-averaged measurements collected inside of a tunnel or by the roadside. Tunnel and roadside measurements can characterize overall fleet-average HONO emissions, but they have two major disadvantages: (1) the measurements are not able to reflect single-vehicle emissions and the effects of emission standards, vehicle types, and fuel types on HONO emissions; and (2) vehicle emissions of HONO can be overestimated because heterogeneous reactions of NO_2 with adsorbed water on the ground surface also generated HONO.[13,25] On the other hand, chassis dynamometer experiments are time-consuming and costly, and as a result, only a small sample size of vehicles can be measured, but it can measure the HONO emissions from individual vehicles under various driving conditions. However, due to the high temperature, humidity, and high HONO concentrations from vehicle exhaust, a constant volume sampler (CVS) is used to dilute the exhaust before it enters the HONO measurement system in the chassis dynamometer experiments.[19,23,27] However, previous CVS may led to significant measurement bias, especially when dilution ratios (DRs) exceed 20.[30] Given the large variations in the HONO concentrations from different vehicles under different driving conditions, it is challenging for the CVS to solve measurement bias due to the limitation of constant volume sampling approach. Thus, we developed a new dilution technique that can resolve the issue of measurement bias under high dilution ratios.

In this study, we, for the first time, directly measure the HONO emissions from light-duty diesel trucks (LDDTs) of different Chinese vehicle emission standards. The challenges in measuring the high concentrations of HONO have been partly overcome by the development of an online portable HONO measurement system featuring the use of a novel dilution technique and the Long-Path Absorption Photometer (LOPAP). This system has a good performance in the dilution ratio and the potential for on-road vehicle emission measurements. This system was adopted in the chassis dynamometer experiments to measure the HONO emissions of 17 light-duty diesel trucks under two widely used test cycles. Sixteen light-duty gasoline vehicles (LDGVs) were also tested to validate our measurement system against results from previous studies on gasoline vehicles. The findings of this study will address the aforementioned gaps in the available HONO emissions data for diesel vehicles and promote a better understanding of HONO sources.

EXPERIMENTAL DESIGN

Portable HONO Emissions Measurement System with a Novel Dilution Technique. Previous experiments usually used CVS with a constant volume dilution method, which led to a high measurement bias and failure to capture large variations in the HONO emissions from vehicles. In this study, we developed a novel portable emissions measurement system (Figure 1a), which included an innovative portable split dilution system (PSDS) and a customized portable HONO

https://dx.doi.org/10.1021/acs.est.0c05599
Environ. Sci. Technol. 2021, 55, 200−208

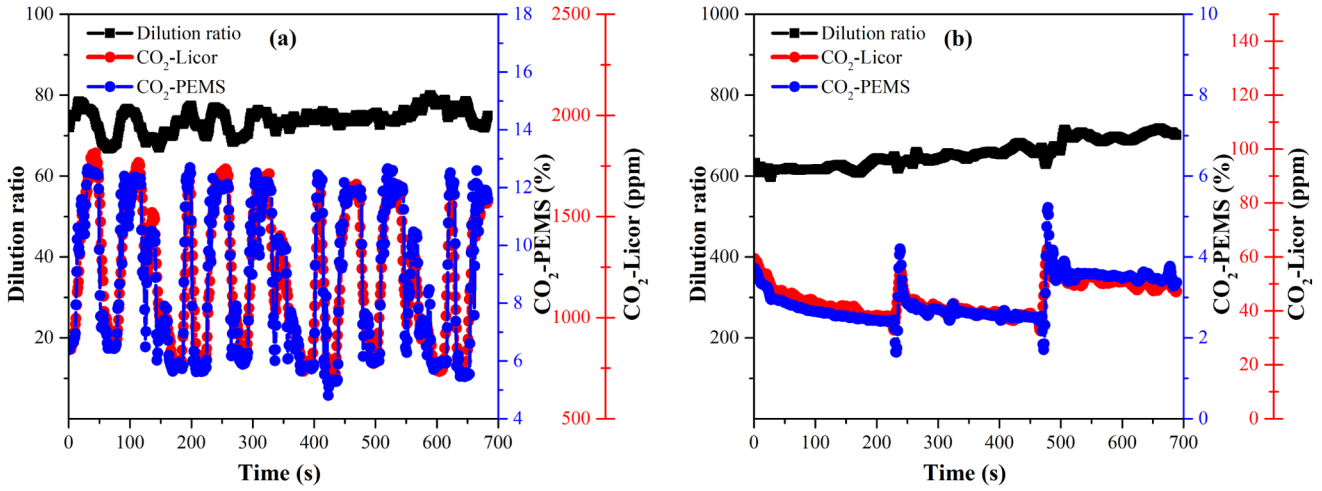

Figure 2. Concentrations of CO_2 and calculated dilution ratio during the measurements of (a) a LDGV based on the ECE cycle and (b) a LDDT based on SSM cycle. The blue lines represent the concentrations of CO_2 measured by PEMS before entering the PSDS. The red lines represent the concentrations of CO_2 measured by the CO_2 analyzer after passing the PSDS. The black lines represent the real-time dilution ratio that is calculated based on eq 1.

emissions measurement system (LOPAP). The systems are able to measure the HONO emissions even at high dilution ratios.

The innovated PSDS adopts a split-flow dilution method that greatly reduces the size of the system and avoids the use of a suction pump and large volumes of dilution gas. To reduce the measurement bias at a high dilution ratio, the system consists of three smaller chambers in series (Figure 1b), which enables the exhaust to be diluted three times to achieve a high dilution ratio. In the PSDS, the sampling tube between the first dilution chamber and the second dilution chamber is heated at a constant temperature (60 °C) to prevent the condensation of exhaust gas, thus avoiding the loss of HONO in the dilution tube. PSDS also reduces the influence of humidity in the HONO measurement, as water vapor is also diluted by a high dilution ratio. Meanwhile, instead of using metal tubes employed in previous studies and ambient air as a diluent, the PSDS adopted Teflon sampling tubes and used nitrogen for the dilution gas. This avoids the loss of HONO to photolysis reactions in the tubes and reduces the impact of any background HONO found in the ambient air on the measurement results. The detailed design of the PSDS is summarized in the Supporting Information (SI). Additionally, to avoid potential system errors of dilution ratio on the measurements, a CO_2 analyzer (Li-840A. Licor, Inc.) is set up after PSDS to calculate the real-time dilution ratio by tracking the CO_2 concentrations before and after dilution. The dilution ratio (DR) is calculated according to eq 1.

$$\mathrm{DR} = \frac{C_{\mathrm{CO_2}}(\mathrm{PEMS})}{C_{\mathrm{CO_2}}(\mathrm{Licor})} \times 10^4 \quad (1)$$

where $C_{\mathrm{CO_2}}(\mathrm{PEMS})$ is the instantaneous CO_2 concentrations (%) measured by a portable emission measurement system (before entering PSDS) and $C_{\mathrm{CO_2}}(\mathrm{Licor})$ is the instantaneous CO_2 concentrations (ppmv) measured by the CO_2 analyzer (after dilution in PSDS).

In addition to the innovated PSDS, we (Jinan University) also developed LOPAP (which is referred to as LOPAP-JNU) based on the Griess colorimetric method to measure the HONO concentrations.[31,32] LOPAP-JNU includes three main modules: the sampling module, the reaction module, and the detection module. LOPAP-JNU has a response time of approximately 90 s, data refresh time of 1 s, and detection limit of approximately 16 pptv. Another LOPAP developed by Peking University (LOPAP-PKU) is also tested to evaluate the performance of LOPAP-JNU (see SI). The LOPAP adjusts two stripping coils in series that can reliably quantify and eliminate the influence of interferences (including NO_2, NO, O_3, SO_2, etc.) on the HONO measurement (see SI), especially for NO_2. In this study, we conducted a laboratory experiment to investigate the interference of high NO_2 concentration before the chassis dynamometer experiment for vehicle exhausts (Figure S1); the results showed the interference of NO_2 could be quantified by the LOPAP instrument. Also, we calibrated the reported HONO concentrations based on the dynamic zero point of interferences. The instantaneous mass emission of HONO (m_{HONO} in the unit of g/min) is calculated according to eq 2.

$$m_{\mathrm{HONO}} = \frac{C_{\mathrm{HONO}} \times V_{\mathrm{HONO}}}{22.4} \times \frac{273}{273 + T} \times M_{\mathrm{HONO}} \times f_{\mathrm{int}} \times V_{\mathrm{EFM}} \times 10^{-9} \quad (2)$$

where C_{HONO} is the instantaneous HONO concentrations (ppbv) measured by LOPAP. V_{HONO} is the gas sampling rate (L/min) of the HONO measurement system. M_{HONO} is the molecular weight of HONO. T is the ambient temperature (°C) at the testing site. V_{EFM} is the gas flow rate (L/min) measured by the exhaust flow meter (EFM). f_{int} is the interference factor of the correction coefficient of collection efficiency in the sampling module.

To understand the relationships between the HONO emissions and regulatory gaseous pollutants, a portable emission measurement system (PEMS) manufactured by SEMTECH-DS (Sensor Inc.) was also directly connected to the EFM. PEMS measures the instantaneous exhaust mass flow rates of the vehicles. The PEMS is used to measure the emissions of the regulatory gaseous pollutants including CO_2, CO, NOx (NO and NO_2), a totalof 147 hydrocarbons (THCs), and the instantaneous exhaust mass flow rates of the vehicles.

https://dx.doi.org/10.1021/acs.est.0c05599
Environ. Sci. Technol. 2021, 55, 200−208

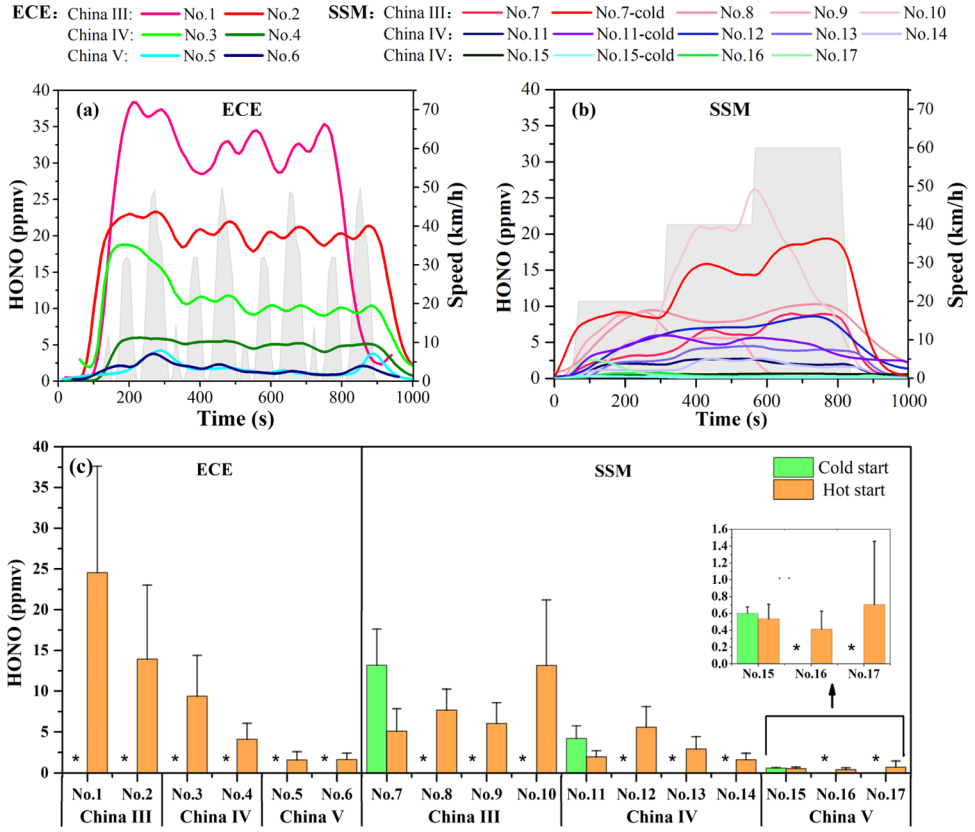

Figure 3. Time series of the HONO concentrations from LDDTs at (a) ECE driving cycle, vehicles 1− 6 and (b) SSM driving cycle, vehicles 7−17. (c) Average HONO concentrations from LDDTs for ECE and SSM driving cycles. Gray shades represent the speeds of driving cycles. The symbols "*" represent "not tested".

Test Vehicles and Driving Conditions. To characterize the HONO emissions from LDDTs under different China emission control standards (equivalent to Euro standards), seventeen LDDTs were randomly selected. The tested LDDTs include vehicles with three emission control standards: China III, China IV, and China V. Detailed specifications of the vehicles are shown in Table S1. Also, considering that the driving conditions may have important influences on HONO emissions, two widely used driving cycles (Figure S2) were adopted in this study: Economic Commission for Europe (ECE) test cycle and a customized steady-state mode (SSM) cycle. The ECE cycle is comprised of four repeated segments to simulate the urban driving conditions, in which the driving speeds change drastically. On the other hand, SSM simulates more stable driving conditions and consists of three different constant speed stages: 20, 40, and 60 km/h, each lasting 4 min. Hot start mode was tested for all LDDTs and cold start mode (parking time > 12 h) was tested for three LDDTs. In addition, 16 LDGVs were tested with the ECE cycle to validate our measurement system against previous studies. The tested LDGVs include vehicles with four emission control standards: China III, China IV, China V, and China VI. Detailed specifications of the vehicles and emission standards are shown in Tables S2 and S4.

RESULTS AND DISCUSSION

Measurement System Performance. To evaluate the stability of PSDS, the time series of CO_2 concentrations (before and after PSDS) and dilution ratio for a tested LDGV and LDDT are illustrated in Figure 2. As shown in Figure 2, the PSDS can stably support both low dilution ratios (73.8 ± 2.8, shown in Figure 2a) and high dilution ratios (655.6 ± 32.4, shown in Figure 2b). In general, the PSDS maintains an excellent performance of dilution ratio (standard deviation: ±5%). Occasionally, sharp changes in pollutant concentrations may cause fluctuations in the dilution ratio, but the PSDS was capable of calculating the real-time dilution ratio based on the CO_2 analyzer so that the dilution ratios used to calculate the HONO concentrations are accurate. This evaluation demonstrates that the PSDS can flexibly and accurately adjust the dilution ratios and is therefore suitable for measuring a wide range of HONO concentrations.

We also evaluated the performance of LOPAP-JNU by conducting comparison experiments using LOPAP-PKU; the results (Figure S3) showed that their measured HONO concentrations are highly consistent (R^2 = 0.97). In addition, to validate our measurement system, we compared the HONO emission concentrations (Figure S4) and emission factors (Figure S5) for the 16 LDGVs measured in this study with previous studies.[23,27] The measured average HONO concentrations in the LDGV exhaust for China III, China IV, China V, and China VI were 54.86 ppbv, 22.26 ppbv, 41.13 ppbv, and 4.18 ppbv, respectively, which are within the range of a few to hundreds of ppbv reported by Nakashima and Kajii. (2017).[23] The $ER_{HONO/NOx}$ for LDGV presented in Table S3 also indicates that our measurement results are consistent with previous studies. In addition, our measured regulatory gaseous pollutants distance-based emission factor (EF) for China III and China IV LDDT were in agreement with previous studies (Figure S6).[33,34] These consistencies with previous studies for

https://dx.doi.org/10.1021/acs.est.0c05599
Environ. Sci. Technol. 2021, 55, 200−208

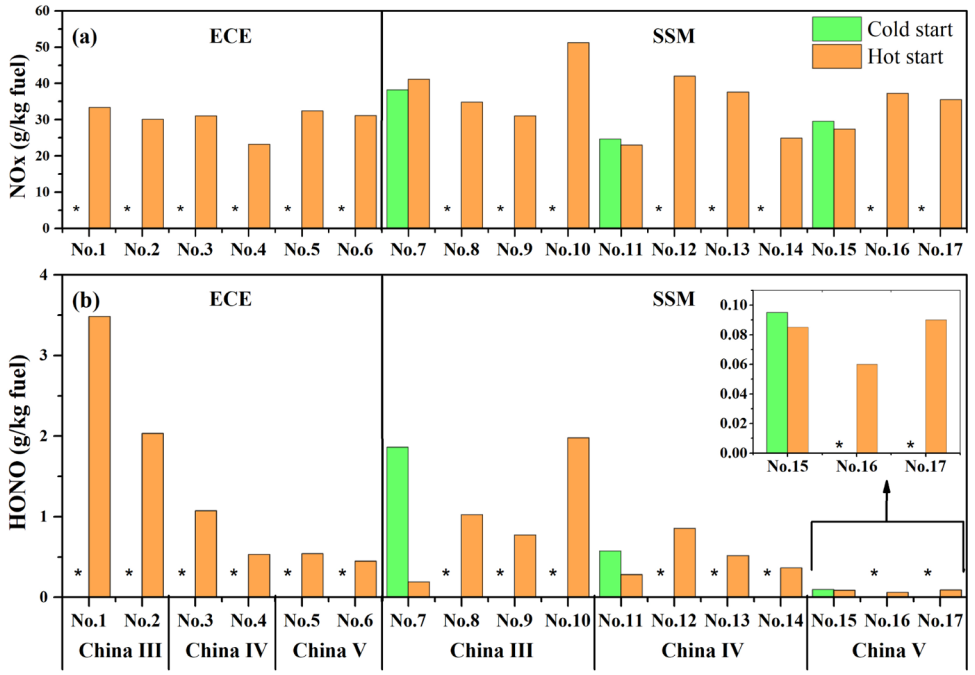

Figure 4. Summary of (a) NO_X and (b) HONO EFs from LDDTs in the tested driving cycle of ECE and SSM. The symbols "*" represent not tested.

Table 1. Comparisons of HONO, NO, and NO_2 Emission Factors among Different Studies

		diesel vehicle			gasoline vehicle		
emission study	standard	HONO (g/kg)	NO (g/kg)	NO_2 (g/kg)	HONO (g/kg)	NO (g/kg)	NO_2 (g/kg)
this study[a]	China III	1.85 ± 1.17	24.79 ± 5.92	12.13 ± 2.66	(1.93 ± 2.76) × 10^{-3}	3.79 ± 2.06	0.11 ± 0.05
	China IV	0.59 ± 0.25	24.16 ± 4.44	6.09 ± 6.16	(8.45 ± 7.57) × 10^{-4}	1.46 ± 0.82	0.09 ± 0.07
	China V	0.15 ± 0.14	32.12 ± 3.28	0.61 ± 0.20	(1.17 ± 1.61) × 10^{-3}	2.77 ± 3.56	0.16 ± 0.05
	China VI				(1.45 ± 0.64) × 10^{-4}	0.84 ± 0.12	0.14 ± 0.01
Kurtenbach[b] et al., 2001[13]		0.12 ± 0.01	11.90 ± 0.70	2.00 ± 0.20	0.094 ± 0.027	8.60 ± 1.70	<0.03
Liu et al., 2017[19]	China IV[c]				(7.00 ± 4.00) × 10^{-4}	0.79 ± 0.14[d]	
Nakashima and Kajii et al., 2017[23]					(0.01−3.60) × 10^{-3}[e]		

[a]Note: All of the values reported in this study are a straight average for all measurements (including both ECE and SSM test cycles). [b]Tunnel study. [c]The tested vehicle is equipped with a gasoline direct injection (GDI) engine. [d]The value is the NOx emission factor. [e]The value is a range.

LDGV and LDDT suggest the reliability of our entire measurement system for regulatory gaseous pollutants and HONO emissions.

HONO Emission Characteristics of LDDT. The time series of HONO emission concentrations and the averaged concentrations from LDDT exhausts are shown in Figure 3. There are obvious emission variations with the fluctuation of speeds; the HONO concentrations rapidly increased during accelerations and dropped sharply during deceleration during both test cycles. As ECE has higher frequencies of accelerations and decelerations, vehicles under the same emission control standard generally have higher HONO emissions for ECE driving cycles than those for the SSM cycles. This is probably because frequent speed changes can lead to incomplete combustion in the engine and promote the HONO formation from NO_2 and intermediate species such as HO_2, CH_2O, and CH_3O,[19,35] indicating that the HONO emissions are sensitive to driving conditions.

As shown in Figure 3c, the start modes and emission control standards are two other important factors influencing the HONO emissions in addition to driving conditions. Overall, the cold start mode was found to emit higher levels of HONO than the hot start mode though only three diesel vehicles were tested for the cold start mode in this study. The same phenomenon was found for 12 out of 14 tested gasoline vehicles (Figure S4). The HONO concentrations decrease with the upgrade of emission standards for both driving cycles. The measured average HONO concentrations are 11 739 ± 6635 ppbv for China III, 4258 ± 2646 ppbv for China IV, and 974 ± 527 ppbv for China V, which are much higher than those (~869 ppbv) reported by Trinh et al. (2017)[27] for a diesel vehicle with an emission standard similar to China IV. Our findings indicate that the HONO concentrations from LDDTs are much higher than the measurements in previous studies.

HONO Emission Factors. We calculated the fuel consumption based EFs of HONO and other gaseous pollutants from LDDTs, which were summarized in Figures 4 and S8, respectively. The emission standard, test cycle, and start mode are found to influence the fuel-based emission factors of HONO from diesel vehicles. The calculated EFs of HONO from China III, China IV, and China V LDDT for the ECE cycle were 3.22 ± 1.23, 0.79 ± 0.27, and 0.32 ± 0.13 g/kg, respectively, while the EFs for the SSM cycle were 1.16 ±

https://dx.doi.org/10.1021/acs.est.0c05599
Environ. Sci. Technol. 2021, 55, 200−208

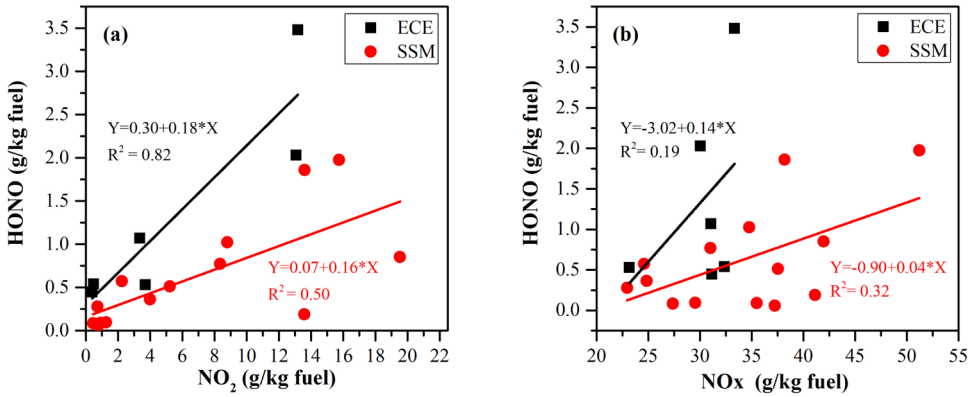

Figure 5. (a) Linear regressions for HONO EFs and NO_2 EFs. (b) Linear regressions for HONO EFs and NOx EFs of LDDTs tested at two driving cycles: ECE cycle (black square) and SSM cycle (red circle).

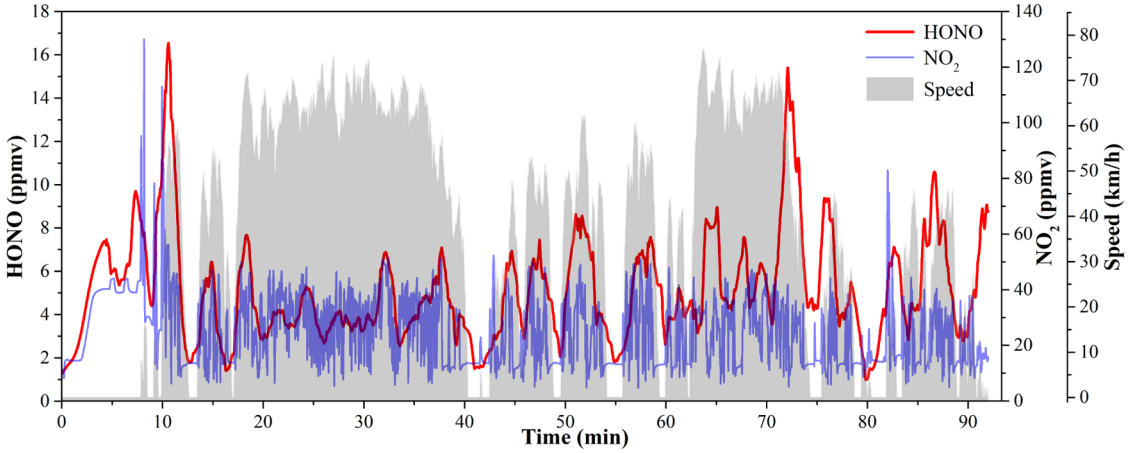

Figure 6. Time series of HONO (red line) and NO_2 (blue line) emissions from a China III heavy-duty diesel truck in an on-road experiment. Gray shades represent the measured second-by-second vehicle speed.

0.48, 0.50 ± 0.22, and 0.078 ± 0.013 g/kg, respectively (Table S5). The HONO EFs for the ECE cycle were found to be higher than those for the SSM cycle, as shown in Figure 4. It should also be noted that the HONO emissions are more susceptible to driving conditions than the emissions of NOx and other gaseous pollutants, as shown in Figures 4 and S8, indicating that accurate measurements of the HONO emissions from LDDTs should take into account the influence of driving conditions of the HONO emissions.

The HONO emission factors of diesel vehicles were found to be 1000 times higher than those of gasoline vehicles of the same emission standard. This is mainly because the heterogeneous conversion of NO_2 on the particles in vehicle exhaust is one major pathway of HONO formation[36,37] and there are generally high NO_2 and particle concentrations in the diesel vehicle exhausts.[38] HONO EFs of the gasoline vehicles measured in our study are consistent with most recent studies, while the HONO EFs of diesel vehicles are significantly higher than those in previous studies (Table 1).

For further comparison of our results with other studies, we calculated the ratio of $ER_{HONO/NOx}$, a parameter that was established by previous measurements and commonly used to estimate the HONO emissions in many modeling studies due to the lack of emission factors. For LDDTs at the SSM cycle, the average $ER_{HONO/NOx}$ from China III to China V were 2.9, 1.5, and 0.27%, respectively. On the other hand, for the ECE cycle, the average $ER_{HONO/NOx}$ from China III to China V were 8.5, 2.8, and 1.0%, respectively. The $ER_{HONO/NOx}$ of most tested diesel vehicles is significantly higher than that reported by previous studies (Table S3).

Correlations between HONO, NO_2, and NOx. In this study, we quantified the correlations between HONO and NOx and HONO and NO_2 emissions, as shown in Figure 5. Intriguingly, there are strong correlations between the HONO and NO_2 emissions at both ECE (R^2 = 0.82) and SSM (R^2 = 0.50) cycles from LDDTs (Figure 5a), which are much higher than those between HONO and NOx emissions with R^2 = 0.19 at the ECE cycle and R^2 = 0.32 at the SSM cycle (Figure 5b). Also, the correlations of the HONO EFs with NO_2 EFs are much higher than those of HONO EFs with the EFs of other pollutants (Figure S9) for LDDTs. However, for gasoline vehicles, the correlations between HONO and NOx emissions as well as HONO and NO_2 emissions are both poor (Figure S10). This might be attributable to the difference in the gas compositions of the exhausts of gasoline and diesel vehicles, such as carbonyl compounds, suggesting that the gas composition could be an important factor influencing the HONO emissions.[35,39,40] Therefore, although the $ER_{HONO/NOx}$ is widely used to estimate the HONO emissions from vehicles when HONO emission factors are not available, the low correlations between HONO and NOx found in this study indicated that such a proxy may bring high uncertainties in estimating the HONO emissions from the vehicles.

https://dx.doi.org/10.1021/acs.est.0c05599
Environ. Sci. Technol. 2021, 55, 200−208

Implications. This study developed a novel portable emission measurement system to directly measure the HONO concentrations from vehicle exhausts and found that there are high HONO emission concentrations from diesel vehicles and the driving condition is one of the important factors affecting the HONO concentrations. Since real-world driving conditions are much more complicated than dynamometer driving cycles, it is expected that the HONO concentrations will vary in an even wider range. Using the portable HONO emission measurement system developed in this study, we conducted a real-world on-road vehicle HONO emission measurement for a China III heavy-duty diesel truck on both highways and nonhighway roads in a suburban area in Guangzhou, China. The second-by-second time-series data of the measured HONO, NO_2, and speed are shown in Figure 6. Compared to dynamometer testing results, as expected, there are significantly fluctuating HONO concentrations (ranging from 2 to 16 ppmv), and the HONO emissions are more sensitive to speed changes than NO_2 emissions. In real-world driving, speed fluctuation, road grade, and even driving behaviors may have great impacts on driving conditions. Thus, to better characterize the HONO emissions from the vehicles and reduce uncertainties in the HONO emission estimates, it is necessary to conduct real-world on-road HONO emission testing for vehicles, especially for diesel vehicles with high HONO emissions. The portable HONO measurement system developed in this study makes on-road testing possible and practical. In fact, with its flexibility in dilution ratio adjustment, this system can also be used to measure the HONO emissions from other sources such as soil and biomass burning to improve our understanding of HONO sources.

In addition, based on online measured NO_2, NOx, and HONO emissions data from gasoline and diesel vehicles, except that there are strong correlations between NO_2 and HONO emissions from diesel vehicles, we found that the correlations between HONO and NOx for both diesel and gasoline vehicles and the correlations between HONO and NO_2 for gasoline vehicles are very poor. These findings implied that the widely used approach, taking the ratio of HONO to NOx ($ER_{HONO/NOx}$, typically 0.8%) to estimate the HONO emissions from vehicles, would be inappropriate and would lead to very high uncertainty in estimating the HONO emissions. Rather than using $ER_{HONO/NOx}$ to infer HONO emissions, directly adopting the HONO emission factors can greatly reduce the uncertainty in the estimates of the HONO emission from vehicles. Thus, we recommend future studies to directly measure the HONO emission factors of mobile sources with the aid of newly available instruments (including those developed in this study) and promote a better understanding of the sources of atmospheric HONO.

■ ASSOCIATED CONTENT

Supporting Information

The Supporting Information is available free of charge at https://pubs.acs.org/doi/10.1021/acs.est.0c05599.

Additional materials and methods, five additional tables (Tables S1−S5), and ten additional figures (Figures S1−S10) (PDF)

■ AUTHOR INFORMATION

Corresponding Author

Junyu Zheng − *Institute for Environmental and Climate Research and Guangdong-Hongkong-Macau Joint Laboratory of Collaborative Innovation for Environmental Quality, Jinan University, Guangzhou 510632, China;* orcid.org/0000-0002-8267-7255; Email: zheng.junyu@gmail.com

Authors

Songdi Liao − *College of Environment and Energy, South China University of Technology, Guangzhou 510641, China*

Jiachen Zhang − *Department of Civil and Environmental Engineering, University of Southern California, Los Angeles, California 90089, United States*

Fei Yu − *Institute for Environmental and Climate Research and Guangdong-Hongkong-Macau Joint Laboratory of Collaborative Innovation for Environmental Quality, Jinan University, Guangzhou 510632, China*

Manni Zhu − *College of Environment and Energy, South China University of Technology, Guangzhou 510641, China*

Junwen Liu − *Institute for Environmental and Climate Research and Guangdong-Hongkong-Macau Joint Laboratory of Collaborative Innovation for Environmental Quality, Jinan University, Guangzhou 510632, China*

Jiamin Ou − *Department of Sociology, Utrecht University, Utrecht 3584 CH, The Netherlands*

Huabin Dong − *College of Environmental Sciences and Engineering, Peking University, Beijing 100871, China*

Qinge Sha − *Institute for Environmental and Climate Research and Guangdong-Hongkong-Macau Joint Laboratory of Collaborative Innovation for Environmental Quality, Jinan University, Guangzhou 510632, China*

Zhuangmin Zhong − *Institute for Environmental and Climate Research and Guangdong-Hongkong-Macau Joint Laboratory of Collaborative Innovation for Environmental Quality, Jinan University, Guangzhou 510632, China*

Yan Xie − *College of Environment and Energy, South China University of Technology, Guangzhou 510641, China*

Haoming Luo − *Institute for Environmental and Climate Research and Guangdong-Hongkong-Macau Joint Laboratory of Collaborative Innovation for Environmental Quality, Jinan University, Guangzhou 510632, China*

Lihang Zhang − *College of Environment and Energy, South China University of Technology, Guangzhou 510641, China*

Complete contact information is available at: https://pubs.acs.org/10.1021/acs.est.0c05599

Notes

The authors declare no competing financial interest.

■ ACKNOWLEDGMENTS

The financial support by the National Natural Science Foundation of China (No. 41627809) and the National Key Research and Development Program of China (No. 2018YFC0213904) are gratefully acknowledged. We acknowledge the support received from all students in our laboratory.

■ REFERENCES

(1) Ren, X.; Harder, H.; Martinez, M.; Lesher, R. L.; Oliger, A.; Simpas, J. B.; Brune, W. H.; Schwab, J. J.; Demerjian, K. L.; He, Y.; Zhou, X.; Gao, H. OH and HO2 Chemistry in the Urban Atmosphere of New York City. *Atmos. Environ.* **2003**, *37*, 3639−3651.

(2) Alicke, B.; Geyer, A.; Hofzumahaus, A.; Holland, F.; Konrad, S.; Pätz, H. W.; Schäfer, J.; Stutz, J.; Volz-Thomas, A.; Platt, U. OH Formation by HONO Photolysis during the BERLIOZ Experiment. *J. Geophys. Res.* **2003**, *108*, 3−1.
(3) Lee, B. H.; Wood, E. C.; Herndon, S. C.; Lefer, B. L.; Luke, W. T.; Brune, W. H.; Nelson, D. D.; Zahniser, M. S.; Munger, J. W. Urban Measurements of Atmospheric Nitrous Acid: A Caveat on the Interpretation of the HONO Photostationary State. *J. Geophys. Res. Atmos.* **2013**, *118*, 12274−12281.
(4) Kleffmann, J. Daytime Sources of Nitrous Acid (HONO) in the Atmospheric Boundary Layer. *ChemPhysChem* **2007**, *8*, 1137−1144.
(5) Stone, D.; Whalley, L. K.; Heard, D. E. Tropospheric OH and HO2 Radicals: Field Measurements and Model Comparisons. *Chem. Soc. Rev.* **2012**, *41*, 6348−6404.
(6) Bao, F.; Li, M.; Zhang, Y.; Chen, C.; Zhao, J. Photochemical Aging of Beijing Urban PM2.5: HONO Production. *Environ. Sci. Technol.* **2018**, *52*, 6309−6316.
(7) Michoud, V.; Colomb, A.; Borbon, A.; Miet, K.; Beekmann, M.; Camredon, M.; Aumont, B.; Perrier, S.; Zapf, P.; Siour, G.; Ait-Helal, W.; Afif, C.; Kukui, A.; Furger, M.; Dupont, J. C.; Haeffelin, M.; Doussin, J. F. Study of the Unknown HONO Daytime Source at a European Suburban Site during the MEGAPOLI Summer and Winter Field Campaigns. *Atmos. Chem. Phys.* **2014**, *14*, 2805−2822.
(8) Cui, L.; Li, R.; Zhang, Y.; Meng, Y.; Fu, H.; Chen, J. An Observational Study of Nitrous Acid (HONO) in Shanghai, China: The Aerosol Impact on HONO Formation during the Haze Episodes. *Sci. Total Environ.* **2018**, *630*, 1057−1070.
(9) Li, D.; Xue, L.; Wen, L.; Wang, X.; Chen, T.; Mellouki, A.; Chen, J.; Wang, W. Characteristics and Sources of Nitrous Acid in an Urban Atmosphere of Northern China: Results from 1-Yr Continuous Observations. *Atmos. Environ.* **2018**, *182*, 296−306.
(10) Pagsberg, P.; Bjergbakke, E.; Ratajczak, E.; Sillesen, A. Kinetics of the Gas Phase Reaction OH + NO (+ M) HONO (+ M) and the Determination of the UV Absorption Cross Sections of HONO. *Chem. Phys. Lett.* **1997**, *272*, 383−390.
(11) Finlayson-Pitts, B. J.; Wingen, L. M.; Sumner, A. L.; Syomin, D.; Ramazan, K. A. The Heterogeneous Hydrolysis of NO2 in Laboratory Systems and in Outdoor and Indoor Atmospheres: An Integrated Mechanism. *Phys. Chem. Chem. Phys.* **2003**, *5*, 223−242.
(12) Su, H.; Cheng, Y. F.; Shao, M.; Gao, D. F.; Yu, Z. Y.; Zeng, L. M.; Slanina, J.; Zhang, Y. H.; Wiedensohler, A. Nitrous Acid (HONO) and Its Daytime Sources at a Rural Site during the 2004 PRIDE-PRD Experiment in China. *J. Geophys. Res.: Atmos.* **2008**, *113*, 1−9.
(13) Kurtenbach, R.; Becker, K. H.; Gomes, J. A. G.; Kleffmann, J.; Lörzer, J. C.; Spittler, M.; Wiesen, P.; Ackermann, R.; Geyer, A.; Platt, U. Investigations of Emissions and Heterogeneous Formation of HONO in a Road Traffic Tunnel. *Atmos. Environ.* **2001**, *35*, 3385−3394.
(14) Liu, Y.; Lu, K.; Li, X.; Dong, H.; Tan, Z.; Wang, H.; Zou, Q.; Wu, Y.; Zeng, L.; Hu, M.; Min, K. E.; Kecorius, S.; Wiedensohler, A.; Zhang, Y. A Comprehensive Model Test of the HONO Sources Constrained to Field Measurements at Rural North China Plain. *Environ. Sci. Technol.* **2019**, *53*, 3517−3525.
(15) Czader, B. H.; Choi, Y.; Li, X.; Alvarez, S.; Lefer, B. Impact of Updated Traffic Emissions on HONO Mixing Ratios Simulated for Urban Site in Houston, Texas. *Atmos. Chem. Phys.* **2015**, *15*, 1253−1263.
(16) Oswald, R.; Behrendt, T.; Ermel, M.; Wu, D.; Su, H.; Cheng, Y.; Breuninger, C.; Moravek, A.; Mougin, E.; Delon, C.; Loubet, B.; Pommerening-Röser, A.; Sörgel, M.; Pöschl, U.; Hoffmann, T.; Andreae, M. O.; Meixner, F. X. HONO Emissions from Soil Bacteria as a Major Source of Atmospheric Reactive Nitrogen. *Science* **2013**, *341*, 1233−1235.
(17) Porada, P.; Tamm, A.; Raggio, J.; Cheng, Y.; Kleidon, A.; Pöschl, U.; Weber, B. Global NO and HONO Emissions of Biological Soil Crusts Estimated by a Process-Based Non-Vascular Vegetation Model. *Biogeosciences* **2019**, *16*, 2003−2031.
(18) Tong, S.; Hou, S.; Zhang, Y.; Chu, B.; Liu, Y.; He, H.; Zhao, P.; Ge, M. Exploring the Nitrous Acid (HONO) Formation Mechanism in Winter Beijing: Direct Emissions and Heterogeneous Production in Urban and Suburban Areas. *Faraday Discuss.* **2016**, *189*, 213−230.
(19) Liu, Y.; Lu, K.; Ma, Y.; Yang, X.; Zhang, W.; Wu, Y.; Peng, J.; Shuai, S.; Hu, M.; Zhang, Y. Direct Emission of Nitrous Acid (HONO) from Gasoline Cars in China Determined by Vehicle Chassis Dynamometer Experiments. *Atmos. Environ.* **2017**, *169*, 89−96.
(20) Huang, R. J.; Yang, L.; Cao, J.; Wang, Q.; Tie, X.; Ho, K. F.; Shen, Z.; Zhang, R.; Li, G.; Zhu, C.; Zhang, N.; Dai, W.; Zhou, J.; Liu, S.; Chen, Y.; Chen, J.; O'Dowd, C. D. Concentration and Sources of Atmospheric Nitrous Acid (HONO) at an Urban Site in Western China. *Sci. Total Environ.* **2017**, *593*−*594*, 165−172.
(21) Zhang, J.; Chen, J.; Xue, C.; Chen, H.; Zhang, Q.; Liu, X.; Mu, Y.; Guo, Y.; Wang, D.; Chen, Y.; Li, J.; Qu, Y.; An, J. Impacts of Six Potential HONO Sources on HOx Budgets and SOA Formation during a Wintertime Heavy Haze Period in the North China Plain. *Sci. Total Environ.* **2019**, *681*, 110−123.
(22) Liang, Y.; Zha, Q.; Wang, W.; Cui, L.; Lui, K. H.; Ho, K. F.; Wang, Z.; Lee, S. C.; Wang, T. Revisiting Nitrous Acid (HONO) Emission from on-Road Vehicles: A Tunnel Study with a Mixed Fleet. *J. Air Waste Manage. Assoc.* **2017**, *67*, 797−805.
(23) Nakashima, Y.; Kajii, Y. Determination of Nitrous Acid Emission Factors from a Gasoline Vehicle Using a Chassis Dynamometer Combined with Incoherent Broadband Cavity-Enhanced Absorption Spectroscopy. *Sci. Total Environ.* **2017**, *575*, 287−293.
(24) Rappenglück, B.; Lubertino, G.; Alvarez, S.; Golovko, J.; Czader, B.; Ackermann, L. Radical Precursors and Related Species from Traffic as Observed and Modeled at an Urban Highway Junction. *J. Air Waste Manage. Assoc.* **2013**, *63*, 1270−1286.
(25) Yang, Q.; Su, H.; Li, X.; Cheng, Y.; Lu, K.; Cheng, P.; Gu, J.; Guo, S.; Hu, M.; Zeng, L.; Zhu, T.; Zhang, Y. Daytime HONO Formation in the Suburban Area of the Megacity Beijing, China. *Sci. China Chem.* **2014**, *57*, 1032−1042.
(26) Xu, Z.; Wang, T.; Wu, J.; Xue, L.; Chan, J.; Zha, Q.; Zhou, S.; Louie, P. K. K.; Luk, C. W. Y. Nitrous Acid (HONO) in a Polluted Subtropical Atmosphere: Seasonal Variability, Direct Vehicle Emissions and Heterogeneous Production at Ground Surface. *Atmos. Environ.* **2015**, *106*, 100−109.
(27) Trinh, H. T.; Imanishi, K.; Morikawa, T.; Hagino, H.; Takenaka, N. Gaseous Nitrous Acid (HONO) and Nitrogen Oxides (NOx) Emission from Gasoline and Diesel Vehicles under Real-World Driving Test Cycles. *J. Air Waste Manage. Assoc.* **2017**, *67*, 412−420.
(28) Kramer, L. J.; Crilley, L. R.; Adams, T. J.; Ball, S. M.; Pope, F. D.; Bloss, W. J. Nitrous Acid (HONO) Emissions under Real-World Driving Conditions from Vehicles in a UK Road Tunnel. *Atmos. Chem. Phys.* **2020**, *20*, 5231−5248.
(29) Kirchstetter, T. W.; Harley, R. A.; Littlejohn, D. Measurement of Nitrous Acid in Motor Vehicle Exhaust. *Environ. Sci. Technol.* **1996**, *30*, 2843−2849.
(30) Allgood, D.; Brown, T.; Samuelsen, S.; Mori, Y. Comparison of Constant-Volume Sampler and Bag Mini-Diluter Emissions Measurements of a Plug-in Hybrid Electric Vehicle. *Int. J. Engine Res.* **2010**, *11*, 283−295.
(31) Heland, J.; Kleffmann, J.; Kurtenbach, R.; Wiesen, P. A New Instrument to Measure Gaseous Nitrous Acid (HONO) in the Atmosphere. *Environ. Sci. Technol.* **2001**, *35*, 3207−3212.
(32) Liu, Y.; Lu, K.; Dong, H.; Li, X.; Cheng, P.; Zou, Q.; Wu, Y.; Liu, X.; Zhang, Y. In situ monitoring of atmospheric nitrous acid based on multi-pumping flow system and liquid waveguide capillary cell. *J. Environ. Sci.* **2016**, *43*, 273−284.
(33) Shen, X.; Yao, Z.; Zhang, Q.; Wagner, D. V.; Huo, H.; Zhang, Y.; Zheng, B.; He, K. Development of Database of Real-World Diesel Vehicle Emission Factors for China. *J. Environ. Sci.* **2015**, *31*, 209−220.

https://dx.doi.org/10.1021/acs.est.0c05599
Environ. Sci. Technol. 2021, 55, 200−208

(34) Yao, Z.; Wu, B.; Wu, Y.; Cao, X.; Jiang, X. Comparison of NOx Emissions from China III and China IV In-Use Diesel Trucks Based on on-Road Measurements. *Atmos. Environ.* **2015**, *123*, 1−8.
(35) Marrodán, L.; Song, Y.; Herbinet, O.; Alzueta, M. U.; Fittschen, C.; Ju, Y.; Battin-Leclerc, F. First Detection of a Key Intermediate in the Oxidation of Fuel + NO Systems: HONO. *Chem. Phys. Lett.* **2019**, 22−26.
(36) Arens, F.; Gutzwiller, L.; Baltensperger, U.; Gäggeler, H. W.; Ammann, M. Heterogeneous Reaction of NO2 on Diesel Soot Particles. *Environ. Sci. Technol.* **2001**, *35*, 2191−2199.
(37) Salgado, M. S.; Rossi, M. J. Flame Soot Generated under Controlled Combustion Conditions: Heterogeneous Reaction of NO2 on Hexane Soot. *Int. J. Chem. Kinet.* **2002**, *34*, 620−631.
(38) Alves, C. A.; Lopes, D. J.; Calvo, A. I.; Evtyugina, M.; Rocha, S.; Nunes, T. Emissions from Light-Duty Diesel and Gasoline in-Use Vehicles Measured on Chassis Dynamometer Test Cycles. *Aerosol Air Qual. Res.* **2015**, *15*, 99−116.
(39) Dong, D.; Shao, M.; Li, Y.; Lu, S.; Wang, Y.; Ji, Z.; Tang, D. Carbonyl emissions from heavy-duty diesel vehicle exhaust in China and the contribution to ozone formation potential. *J. Environ. Sci.* **2014**, *26*, 122−128.
(40) Li, X.; Hofzumahaus, A.; Brauers, T.; Haseler, R.; Bohn, B.; Broch, S.; Fuchs, H.; Gomm, S.; Holland, F.; Jager, J.; Kaiser, J.; Keutsch, F. N.; Lohse, I.; Lu, K.; Tillmann, R.; Wegener, R.; Wolfe, G.; Mentel, T. F.; Kiendler-Scharr, A.; Wahner, A. Missing Gas-Phase Source of HONO Inferred from Zeppelin Measurements. *Science* **2014**, *344*, 292−297.

https://dx.doi.org/10.1021/acs.est.0c05599
Environ. Sci. Technol. 2021, 55, 200−208